



HAL
open science

Effect of the DNA Polarity on the Relaxation of Its Electronic Excited States

Vasilis Petropoulos, Lorenzo Uboldi, Margherita Maiuri, Giulio Cerullo, Lara Martinez-Fernandez, Evangelos Balanikas, Dimitra Markovitsi

► **To cite this version:**

Vasilis Petropoulos, Lorenzo Uboldi, Margherita Maiuri, Giulio Cerullo, Lara Martinez-Fernandez, et al.. Effect of the DNA Polarity on the Relaxation of Its Electronic Excited States. *Journal of Physical Chemistry Letters*, 2023, 14, pp.10219-10224. 10.1021/acs.jpcclett.3c02580 . hal-04276896

HAL Id: hal-04276896

<https://hal.science/hal-04276896>

Submitted on 9 Nov 2023

HAL is a multi-disciplinary open access archive for the deposit and dissemination of scientific research documents, whether they are published or not. The documents may come from teaching and research institutions in France or abroad, or from public or private research centers.

L'archive ouverte pluridisciplinaire **HAL**, est destinée au dépôt et à la diffusion de documents scientifiques de niveau recherche, publiés ou non, émanant des établissements d'enseignement et de recherche français ou étrangers, des laboratoires publics ou privés.

Effect of the DNA Polarity on the Relaxation of its Electronic Excited States

Vasilis Petropoulos,^a Lorenzo Ubaldi,^a Margherita Maiuri,^a Giulio Cerullo,^{a} Lara Martinez-Fernandez,^{b*} Evangelos Balanikas^c and Dimitra Markovitsi^{d*}*

^a IFN-CNR, Dipartimento di Fisica, Politecnico di Milano, Piazza Leonardo da Vinci 32, I-20133 Milano, Italy; ^b Departamento de Química, Facultad de Ciencias and Institute for Advanced Research in Chemical Sciences (IADCHEM) Universidad Autónoma de Madrid, Campus de Excelencia UAM-CSIC, Cantoblanco, 28049 Madrid, Spain; ^c Department of Physical Chemistry, University of Geneva, CH-1211 Geneva-4, Switzerland; ^d Université Paris-Saclay, CNRS, Institut de Chimie Physique, UMR8000, 91405 Orsay, France

AUTHOR INFORMATION

Corresponding Authors

giulio.cerullo@polimi.it, lara.martinez@uam.es, dimitra.markovitsi@universite-paris-saclay.fr

ABSTRACT

The DNA polarity, *i.e.* the order in which nucleobases are connected together via the phosphodiester backbone, is crucial for several biological processes. But, so far, there has not been experimental evidence regarding its effect on the relaxation of DNA electronic excited states. Here we examine this aspect for two dinucleotides containing adenine and guanine: 5'-dApdG-3' and 5'-dGpdA-3' in water. We used two different femtosecond transient absorption setups, one providing high temporal resolution and broad spectral coverage (330-650 nm) between 30 fs and 50 ps, the other recording decays at selected wavelengths till 1.2 ns. The transient absorption spectra corresponding to the minima in the potential energy surface of the first excited state were computed by quantum chemistry methods. Our results show that the excited charge transfer state in 5'-dGpdA-3' is formed with a quantum yield ~75% higher and slower decay (170±10 ps vs 112±12 ps) compared to 5'-dApdG-3'.

The polarity of nucleic acids, that is the order according to which two adjacent nucleobases are linked together within a strand via the phosphodiester backbone, from the 5' end to the 3' end,¹ determines the adopted conformations,²⁻⁴ and play a key role in biological functions depending on structural features.⁵⁻⁸ Among others, it has been reported that the DNA/RNA strand polarity has an influence on processes involving various redox reactions,⁹⁻¹² as well as hole transport in DNA.¹³ A transfer of an electrical charge takes also place between stacked nucleobases following absorption of UV radiation by DNA, leading to population of excited charge transfer (CT) states. Femtosecond transient absorption studies showed that, in DNA multimers, an important part of the initially excited state population evolves toward CT states.¹⁴⁻²² The latter survive much longer, up to several hundreds of ps, while the monomer excited states decay within, at most, 10 ps.

Theoretical studies predicted that CT states should be affected by the strand polarity,²³⁻²⁹ which determines the relative orientation of the stacked nucleobases and, hence, the associated orbital overlap (Figure 1a). Here, focusing on dinucleotides composed of adenine and guanine, we provide the first experimental evidence for such an asymmetrical behavior. We show that the spectral and dynamical features determined for 5'-dApdG-3' (abbreviated as AG) differ from those of 5'-dGpdA-3' (abbreviated as GA), the latter configuration favoring the formation of CT states and slowing down their decay rate. These observations are supported by quantum chemistry computations performed for the same systems.

AG and GA, purified by reversed phase HPLC and tested by MALDI-TOF (Figure S1 in the Supporting Information, SI), were purchased from Eurogentec. They were dissolved in high concentration phosphate buffer ($\sim 0.12 \text{ molL}^{-1}$, pH 7.0), so as to promote stacking, and subsequently excited at 266 nm (Figure 1b). Their transient absorption spectra were recorded from 330 to 650 nm for delays reaching 50 ps by means of a homemade pump-probe setup (I) with a time resolution of 30 fs, already used for the study of DNA.³⁰ The long-time decays were determined in the visible by means of a second setup (II) allowing measurements till 1.2 ns with a time resolution of 100 fs, after checking that the signals obtained with both setups overlap in the 0.1 – 50 ps range (Figure S2). To avoid photodegradation, 6 mL of the solution were kept flowing through a quartz cell whose optical path-length was 1 mm. The concentration of absorbed photons ($8 \times 10^{-6} \text{ molL}^{-1}$) was much lower than the dinucleotide concentration ($2-3 \times 10^{-4}$

molL⁻¹), making two-photon excitation highly improbable. More experimental details are given in the SI.

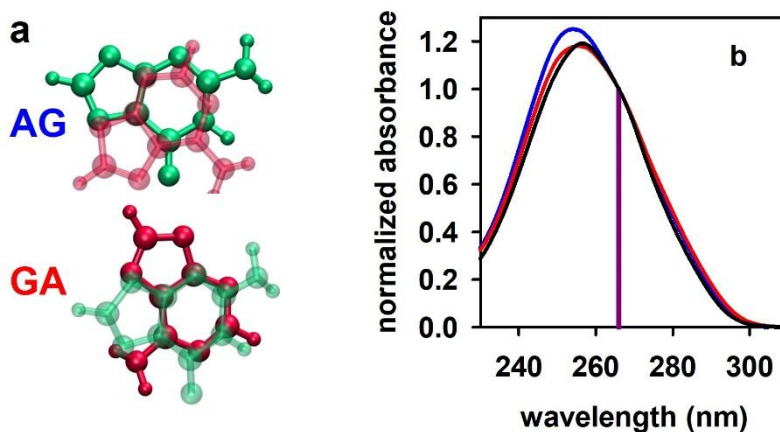


Figure 1. (a) Schematic representation of the geometrical arrangement adopted by the adenine (red) and guanine (green) moieties in the ground state of AG and GA. (b) Steady-state absorption spectra of AG (blue), GA (red) and an equimolar mixture of dAMP and dGMP (black).³¹ The vertical violet line indicates the excitation wavelength used for the transient absorption experiments, 266 nm, at which the spectra have been normalized.

The dinucleotide steady-state absorption spectra are slightly blue-shifted with respect to that of an equimolar mixture of the mononucleotides dAMP and dGMP³¹ (Figure 1b), suggesting some chromophore interaction in the ground state. Thus, their time-resolved behavior should result from an ensemble of configurations, ranging from unstacked chromophores to fully stacked ones. In the limiting case of non-interacting nucleobases, monomer-like decays are expected. The transient absorption spectra of the adenosine and guanosine chromophores are shown in Figure 1c. The former,^{21,30} exhibits two well defined peaks, at 375/380 and 640/685 nm.^{19,28} In contrast, only one intense band, peaking around 300 nm, is present in the latter.³²⁻³³ Adenosine decays much faster than guanosine, with the time needed for the intensity of their UV transient absorption band to decrease by a factor of 10 being, respectively, 1 and 8 ps.^{30,32}

The behavior of the AG and GA dinucleotides considered here, in which the nucleobases are stacked in the ground state was rationalized with the help of quantum chemistry calculations in a previous publication.²⁹ In that theoretical study the entire system (two nucleobases, the connecting backbone and the counter ion), embedded in water through a polarizable continuum model, was taken into account. The relative position of the nucleobases in the ground state of

each system, derived from geometry optimization, is depicted schematically in Figure 1a. The stacking distance is comparable in both systems, around 3.2 Å. Computations provided various minima in the potential energy surface of the first excited state.²⁹ For both systems, a $\pi\pi^*$ state (La) localized on the guanine as well as a $G^{\delta+} \rightarrow A^{\delta-}$ CT state were identified, with δ being equal to 0.5 a.u. for AG and 0.7 a.u. for GA.²⁹ Furthermore, a $\pi\pi^*$ exciton state, delocalized over the adenine and the guanine, was found only for AG.²⁹

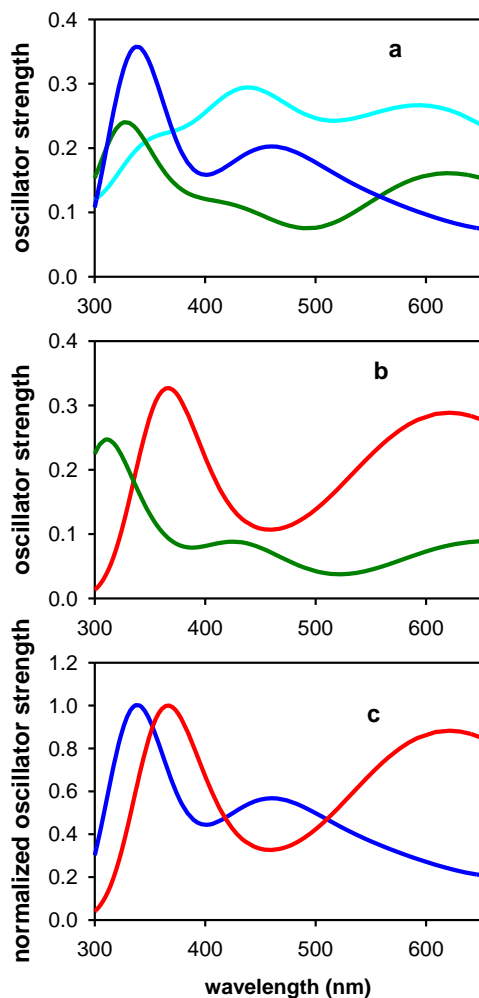


Figure 2. Transient absorption spectra computed for the minima identified in the potential energy surface of the first excited state of AG (a) and GA (b); green: $\pi\pi^*$ state localized on G; cyan: exciton state delocalized over A and G; blue: CT state in AG; red: CT state in GA; the spectra of the CT states are compared in (c) after normalization of their intensity at the UV peak.

In the present study, we computed the transient absorption spectra corresponding to the above-mentioned minima (Figures 2a and 2b). To this end, we used a multifunctional analyzer (multiwfn program)³⁴ to obtain the excited-excited state transition dipole moments. Additional computational details are provided in the SI. The spectra computed for the $\pi\pi^*$ localized excited states are characterized by an intense peak in the UV, a shoulder around 400 nm and a weak intensity band peak above 600 nm. Despite these similarities, subtle differences among the spectra of the two systems can be observed: the UV band of AG is slightly red-shifted ($\lambda_{\text{max}} = 338$ nm) compared with that of GA ($\lambda_{\text{max}} = 312$ nm), while the red band is more intense for the former system. The spectrum of the AG exciton is very broad, extending all over the examined spectral domain, its intensity peaking in the 400 – 450 nm region. Regarding the spectra of the CT states, the UV band is more intense for AG and is located at shorter wavelengths (337 nm vs 367 nm) compared to the one of GA; in addition, the AG band in the visible is less intense and blue shifted with respect to that of GA. The spectra of the CT states, normalized at their maximum, are compared in Figure 2c.

Based on the observations on the excited state relaxation of the non-interacting adenosine and guanosine chromophores in neutral aqueous solution,^{21, 30, 32-33} and considering the theoretical predictions for the excited state relaxation of dinucleotides with fully stacked chromophores, we examine below the experimental transient absorption spectra obtained for AG and GA. The spectral evolution is shown in Figure 3 and, not surprisingly, it is quite complex. The spectra recorded between 100 fs and 1 ps exhibit an intense UV band and a second broader and less intense one peaking in the 580 – 600 nm region (Figures 3a and 3b). During this time interval, the UV band shifts to shorter wavelengths. The same thing happens with the band in the visible, with the exception of an initial red shift between 100 and 200 fs. To better distinguish subsequent changes, which are not accompanied by an important modification of the signal intensity, the spectra obtained between 0.5 and 15 ps have been normalized at their maximum (Figures 3c and 3d). In this time window, it appears that the UV band is composed in fact of two components. The high energy one, located below 350 nm, disappears within ~15 ps. In parallel, the relative intensity of the band in the visible increases and eventually it becomes preponderant. At longer times, no further spectral changes, within the experimental error, could be detected.

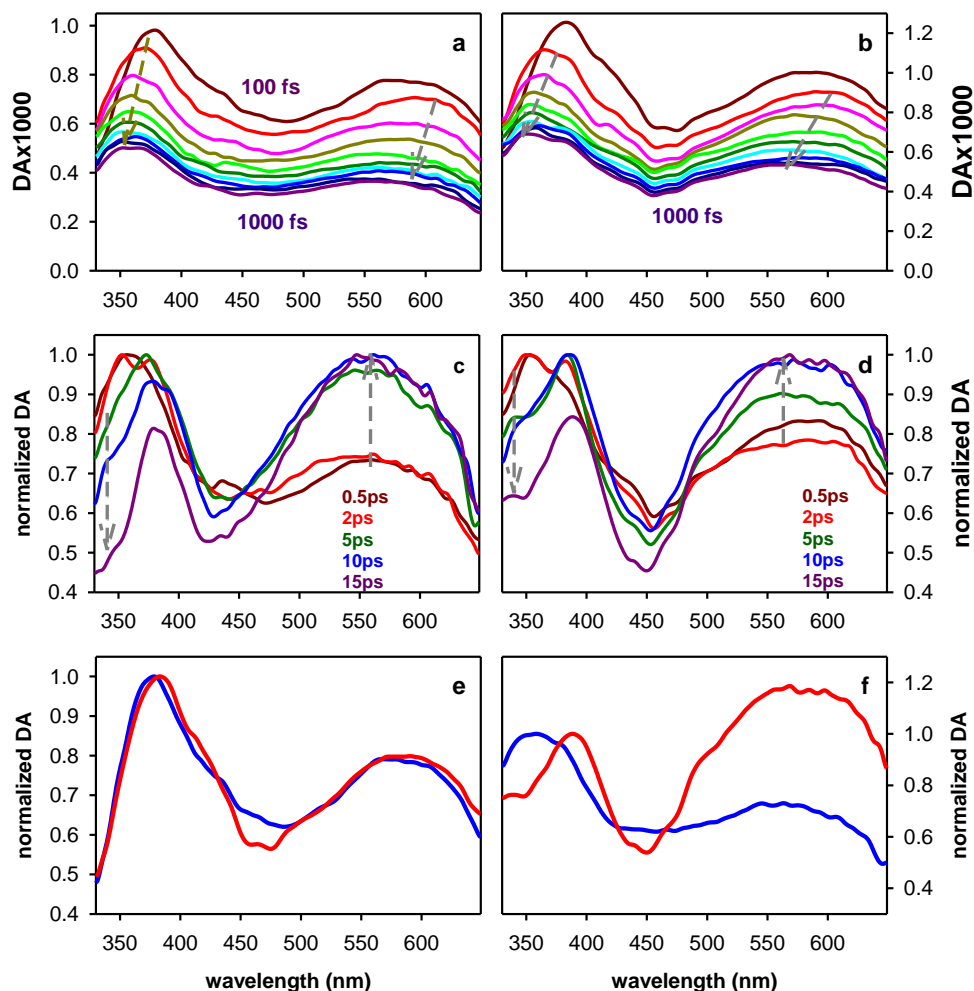


Figure 3. Transient absorption spectra recorded for AG (a and c) and GA (b and d); the spectra in (a) and (b) are recorded from 100 fs to 1 ps with 100 fs steps; the spectra in (c) and (d) are normalized in their maximum. The spectra of AG (blue) and GA (red) at 100 fs and 15 ps, normalized at the UV peak, are compared in (e) and (f), respectively.

We assign the blue shift of the bands in the UV and the visible occurring before 1 ps to the decay of the adenosine $\pi\pi^*$ state (L_a),^{21, 30, 35-36} whose photo-induced absorption spectrum peaks at longer wavelengths compared to that of guanosine (Figure 1c). The disappearance of the high energy component in the UV band, taking place within a few ps, is associated with the decay of the guanosine $\pi\pi^*$ state (Figure 1c).³²⁻³³ The small, albeit detectable, red shift of the band in the visible between 100 and 200 fs is tentatively attributed to exciton states associated with various

configurations. In general, they are expected to undergo fast localization in such flexible systems.

Although the trends described in the previous paragraph are common for AG and GA, there are noticeable differences in both the spectral and the dynamical features of the two systems. Their spectra recorded at 100 fs, expected to correspond mainly to $\pi\pi^*$ states, look quite similar (Figure 3e). The largest difference is observed around 450 nm, where the relative intensity of the AG spectrum is higher. We are tempted to correlate this specific feature with the absorption of the exciton state identified only for AG, exhibiting a characteristic band in this spectral range (Figure 2a). However, as numerous transients enter into play, we cannot be conclusive about this assignment.

At 1 ps the high-energy peak is located at 353 nm for AG vs 349 nm for GA, in line with the relative position of the computed spectra for the excited states localized on the guanosine chromophore (Figures 2a and 2b). The difference between the transient absorption spectra of the two dinucleotides increases with time.

Focusing on the dynamical aspects, the signal at 330 nm, associated mainly with the decay of the guanosine $\pi\pi^*$ state, is faster for AG than for GA (Figure 4a). This could be attributed to a faster formation of the CT state in the former system. This difference in the dynamics is also reflected in the spectra shown in Figures 3c and 3d: the inversion in the relative intensity of the two bands takes place earlier for AG compared to GA.

We judge that, at short times, fits of the decays with multiexponential functions are inappropriate, due to the structural inhomogeneity of the studied systems and the anisotropic reactions taking place. In this respect, we recall that the decays of the free adenosine or guanosine in aqueous solution have been fitted with two or three exponentials each, the time constants depending on the probing wavelength and differing from one study to the other.^{21, 30, 32-33, 37} In any way, it is safe to consider that at 15 ps, all $\pi\pi^*$ states, both localized and excitonic, have disappeared and only the CT states are left. The signals recorded for AG and GA at selected wavelengths between 500 and 645 nm are well described by mono-exponential functions (Figures 4b and 4c). The time constants derived from these fits fall, respectively, in the range of 112 ± 12 ps and 170 ± 10 ps. The former value is in good agreement with the lifetimes reported previously for AG exciplexes (105 ± 30 ps³⁸ and 124 ± 12 ps³⁹) by transient absorption experiments probing in the UV/visible. A more recent study, performed for both AG and GA

probing in the infrared spectral domain, provided much longer lifetimes: 420 ± 120 ps for AG and 280 ± 160 ps for GA.²² As the error bars were quite large, the authors concluded that they could not discriminate between the two systems.

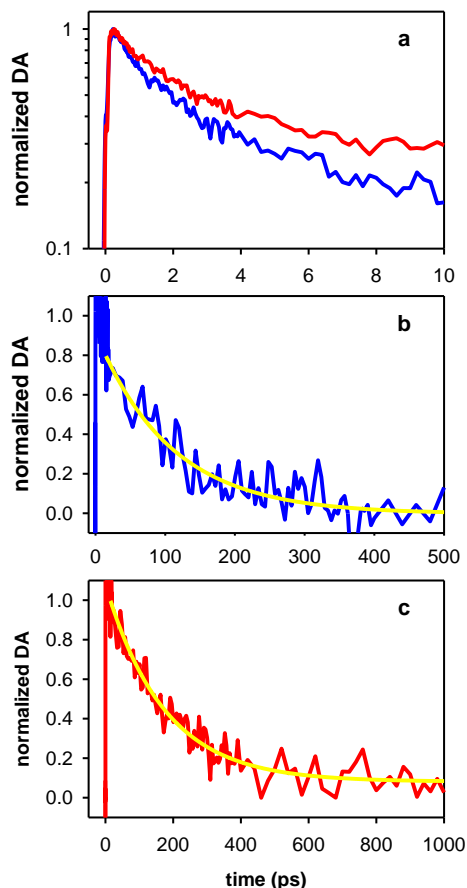


Figure 4. Decays recorded for AG (blue) and GA (red) at 330 nm (a) and 500 nm (b) and (c). The signals in (a) are normalized at their maximum and those in (b) and (c) at 15 ps. Yellow lines correspond to fits with mono-exponential functions.

From the above-described dynamical behavior, we conclude that the spectra at 15 ps, shown in Figure 3f after normalization at their UV peak, correspond to a single transient species, attributed to the CT state. Both spectra exhibit a UV band, peaking at 379 and 390 nm for AG and GA, respectively, and a broader and more intense one appearing at wavelengths longer than 500 nm. The determination of the exact position of the latter band is hampered by a bandpass filter (300 – 630nm) used to eliminate the scattered pump light. Despite this caveat, it is clear that the GA band is red-shifted in respect with that of AG. The relative position of both bands determined

experimentally for the two dinucleotides is reminiscent of what is observed for the computed spectra of their CT states (Figure 2c): both bands of AG are located at shorter wavelengths compared to those of GA.

Although the present measurements do not allow the determination of absolute quantum yields associated with the formation of CT states in each dinucleotide, it is possible to estimate the relative quantum yields of their formation in the two systems. Considering that, under our experimental conditions, the same number of photons is absorbed by either system, the CT concentration in each system is determined by the intensity of the corresponding “zero-time” transient absorption spectrum. The latter are obtained from the transient absorption spectra at 15 ps and the lifetimes of the CT states, as explained in the SI. These “zero-time” spectra of the CT states are shown in Figure S3a. We remark that the intensity of the UV band, for which the experimental error is smaller compared to that of the band in the red, is *ca.* 75% higher for GA than for AG. This difference is unlikely to arise from larger values of the molar extinction coefficients. As a matter of fact, according to the computed spectra (Figure S3b), the maximum oscillator strength of the UV peak is 20% smaller for GA than for AG. Therefore, it appears the CT state is formed with a significantly higher quantum yield in the former system. The relative values of quantum yields can be explained, in part, by the more efficient coupling between CT and $\pi\pi^*$ states in the Franck-Condon region in GA,²⁹ as well as by the presence of an additional relaxation pathway in AG leading to the exciton.

In conclusion, our joint experimental and theoretical study provided clear evidence about the different behavior of the excited state relaxation in the AG and GA dinucleotides, highlighting the influence of the DNA polarity on the CT states. The CT state in AG is formed faster and with a significantly lower quantum yield, absorbs at shorter wavelengths and decays faster compared to what is observed for its counterpart in GA. From a methodological point of view, this is the first time that computed spectra have been used to discriminate among transient species in DNA multimers determined by femtosecond spectroscopy.

It is worth-noticing that our results obtained upon DNA excitation are in line with those observed for redox reactions between ground state DNA and an external oxidant: they are all favored when guanines are located at 5' ends.^{9, 12} Moreover, the catalytic activity of G4-DNAzymes increases with the availability of guanines at 5' ends.¹⁰⁻¹¹ Finally, the present study shed light on the multistep mechanism underlying low-energy photoionization of DNA, proposed

to involve formation of CT states, charge separation and electron ejection by the nucleobase bearing the negative charge.³⁸⁻³⁹ The *ca.* 30% higher photoionization quantum yield determined at 266 nm for guanine quadruplexes composed of four DNA strands 5'-GGGGA-3' (12.6×10^{-3}) compared to 5'-AGGGG-3' strands (9.9×10^{-3}),²⁹ can be explained by the formation of higher concentration of $G^+ \rightarrow A^-$ CT states in the former system, accompanied by a longer lifetime, favoring charge separation and trapping of the electron hole by the stacked guanines.⁴⁰

Supporting Information. Sample details; transient absorption setups; relative quantum yields of CT states; computational details.

ACKNOWLEDGMENT

This work received funding by the European Program H2020 MSCA ITN (grant No. 765266 – LightDyNAMics project)

REFERENCES

1. Alberts, B.; Johnson, A.; Lewis, J.; Raff, M.; Roberts, K.; Walter, P. The Structure and Function of DNA. In *Molecular biology of the cell*, 4th ed.; Garland Science: New York, 2002.
2. Hazel, P.; Huppert, J.; Balasubramanian, S.; Neidle, S. Loop-length-dependent folding of G-quadruplexes. *J. Am. Chem. Soc.* **2004**, *126*, 16405-16415.
3. Bansal, A.; Prasad, M.; Roy, K.; Kukreti, S. A short GC-rich palindrome of human mannose receptor gene coding region displays a conformational switch. *Biopolymers* **2012**, *97*, 950-962.
4. Sket, P.; Korbar, T.; Plavec, J. Influence of 3'-3' inversion of polarity site within d(TGGGGT) on inter quartet cation binding. *J. Mol. Struct.* **2014**, *1075*, 49-52.
5. Gupta, R. C.; Golub, E. I.; Wold, M. S.; Radding, C. M. Polarity of DNA strand exchange promoted by recombination proteins of the RecA family. *Proc. Natl. Acad. Sci. U.S.A.* **1998**, *95*, 9843-9848.
6. de Laat, W. L.; Appeldoorn, E.; Sugawara, K.; Weterings, E.; Jaspers, N. G. J.; Hoeijmakers, J. H. J. DNA-binding polarity of human replication protein A positions nucleases in nucleotide excision repair. *Genes Dev.* **1998**, *12*, 2598-2609.
7. Balasingham, S. V.; Zegeye, E. D.; Homberset, H.; Rossi, M. L.; Laerdahl, J. K.; Bohr, V. A.; Tonjum, T. Enzymatic Activities and DNA Substrate Specificity of Mycobacterium tuberculosis DNA Helicase XPB. *Plos One* **2012**, *7*.
8. Lin, Y. H.; Chu, C. C.; Fan, H. F.; Wang, P. Y.; Cox, M. M.; Li, H. W. A 5-to-3 strand exchange polarity is intrinsic to RecA nucleoprotein filaments in the absence of ATP hydrolysis. *Nucl. Ac. Res.* **2019**, *47*, 5126-5140.
9. Saito, I.; Takayama, M.; Sugiyama, H.; Nakatani, K. Photoinduced DNA Cleavage via Electron Transfer - Demonstration that Guanine Residues located 5' to Guanine are the Most Electron-donating sites. *J. Am. Chem. Soc.* **1995**, *117*, 6406-6407.

10. Virgilio, A.; Esposito, V.; Lejault, P.; Monchaud, D.; Galeone, A. Improved performances of catalytic G-quadruplexes (G4-DNAzymes) via the chemical modifications of the DNA backbone to provide G-quadruplexes with double 3'-external G-quartets. *Int. J. Biol. Macromol.* **2020**, *151*, 976-983.
11. Cao, Y. W.; Li, W. J.; Pei, R. J. Manipulating the Assembly of DNA Nanostructures and Their Enzymatic Properties by Incorporating a 5'-5' Polarity of Inversion Site in the G-Tract. *ACS Macro Lett.* **2021**, *10*, 1359-1364.
12. O'Neill, M. A.; Barton, J. K. Effects of strand and directional asymmetry on base-base coupling and charge transfer in double-helical DNA. *Proc. Natl. Acad. Sci. USA* **2002**, *99*, 16543-16550.
13. Voityuk, A. A.; Jortner, J.; Bixon, M.; Rösch, N. Electronic coupling between Watson-Crick pairs for hole transfer and transport in desoxyribonucleic acid. *J. Chem. Phys.* **2001**, *114*, 5614-5620.
14. Chen, J.; Zhang, Y.; Kohler, B. Excited states in DNA strands investigated by ultrafast laser spectroscopy. *Top. Curr. Chem.* **2015**, *356*, 39-87.
15. Schreier, W. J.; Gilch, P.; Zinth, W. Early Events of DNA Photodamage. *Annu. Rev. Phys. Chem.* **2015**, *66*, 497-519.
16. Kwok, W. M.; Ma, C. S.; Phillips, D. L. "Bright" and "Dark" excited states of an alternating AT oligomer characterized by femtosecond broadband spectroscopy. *J. Phys. Chem. B* **2009**, *113*, 11527-11534.
17. Keane, P. M.; Wojdyla, M.; Doorley, G. W.; Kelly, J. M.; Parker, A. W.; Clark, I. P.; Greetham, G. M.; Towrie, M.; Magno, L. M.; Quinn, S. J. Long-lived excited states in i-motif DNA studied by picosecond time-resolved IR spectroscopy. *Chem. Comm.* **2014**, *50*, 2990-2992.
18. Doorley, G. W.; Wojdyla, M.; Watson, G. W.; Towrie, M.; Parker, A. W.; Kelly, J. M.; Quinn, S. J. Tracking DNA Excited States by Picosecond-Time-Resolved Infrared Spectroscopy: Signature Band for a Charge-Transfer Excited State in Stacked Adenine-Thymine Systems. *J. Phys. Chem. Lett.* **2013**, *4*, 2739-2744.
19. Doorley, G. W.; McGovern, D. A.; George, M. W.; Towrie, M.; Parker, A. W.; Kelly, J. M.; Quinn, S. J. Picosecond transient infrared study of the ultrafast deactivation processes of electronically excited B-DNA and Z-DNA forms of [poly(dG-dC)]₂. *Angew. Chem. Int. Ed.* **2009**, *48*, 123-127.
20. Ma, C. S.; Chan, R. C.-T.; Chan, C. T.-L.; Wong, A. K.-W.; Kwok, W.-M. Real-time Monitoring Excitation Dynamics of Human Telomeric Guanine Quadruplexes: Effect of Folding Topology, Metal Cation, and Confinement by Nanocavity Water Pool. *J. Phys. Chem. Lett.* **2019**, *10*, 7577-7585.
21. Kwok, W.-M.; Ma, C.; Phillips, D. L. Femtosecond time- and wavelength-resolved fluorescence and absorption study of the excited states of adenosine and an adenine oligomer. *J. Am. Chem. Soc.* **2006**, *128*, 11894-11905.
22. Kufner, C. L.; Zinth, W.; Bucher, D. B. UV-Induced Charge-Transfer States in Short Guanosine-Containing DNA Oligonucleotides. *Chembiochem* **2020**, *21*, 2306-2310.
23. Colon, L.; Crespo-Hernandez, C. E.; Oyola, R.; Garcia, C.; Arce, R. Role of sequence and conformation on the photochemistry and the photophysics of A-T DNA dimers: An experimental and computational approach. *J. Phys. Chem. B* **2006**, *110*, 15589-15596.
24. Santoro, F.; Barone, V.; Lami, A.; Improta, R. The excited electronic states of adenine-guanine stacked dimers in aqueous solution: a PCM/TD-DFT study. *Phys. Chem. Chem. Phys.* **2010**, *12*, 4934-4948.

25. Aquino, A. J. A.; Nachtigallova, D.; Hobza, P.; Truhlar, D. G.; Hattig, C.; Lischka, H. The Charge-Transfer States in a Stacked Nucleobase Dimer Complex: A Benchmark Study. *J. Comput. Chem.* **2011**, *32*, 1217-1227.
26. Martinez-Fernandez, L.; Improta, R. Novel adenine/thymine photodimerization channels mapped by PCM/TD-DFT calculations on dApT and TpdA dinucleotides. *Photochem. Photobiol. Sci* **2017**, *16*, 1277-1283.
27. Martinez-Fernandez, L.; Improta, R. Sequence dependence on DNA photochemistry: a computational study of photodimerization pathways in TpdC and dCpT dinucleotides. *Photochem. Photobiol. Sci* **2018**, *17*, 586-591.
28. Lee, W.; Matsika, S. Role of charge transfer states into the formation of cyclobutane pyrimidine dimers in DNA. *Faraday Disc.* **2019**, *216*, 507-519.
29. Balanikas, E.; Martinez-Fernandez, L.; Improta, R.; Podbevsek, P.; Baldacchino, G.; Markovitsi, D. The Structural Duality of Nucleobases in Guanine Quadruplexes Controls Their Low-Energy Photoionization. *J. Phys. Chem. Lett.* **2021**, *12*, 8309-8313.
30. Borrego-Varillas, R.; Cerullo, G.; Markovitsi, D. Exciton Trapping Dynamics in DNA Multimers. *J. Phys. Chem. Lett.* **2019**, *10*, 1639-1643.
31. Onidas, D.; Markovitsi, D.; Marguet, S.; Sharonov, A.; Gustavsson, T. Fluorescence properties of DNA nucleosides and nucleotides: a refined steady-state and femtosecond investigation. *J. Phys. Chem. B* **2002**, *106*, 11367-11374.
32. Karunakaran, V.; Kleinermanns, K.; Improta, R.; Kovalenko, S. A. Photoinduced dynamics of guanosine monophosphate in water from broad-band transient absorption spectroscopy and quantum-chemical calculations. *J. Am. Chem. Soc.* **2009**, *131*, 5839-5850.
33. Cheng, C. C.-W.; Ma, C.; Chan, C. T.-L.; Ho, K. Y.-F.; Kwok, W.-M. The solvent effect and identification of a weakly emissive state in nonradiative dynamics of guanine nucleosides and nucleotides - a combined femtosecond broadband time-resolved fluorescence and transient absorption study. *Photochem. Photobiol. Sci.* **2013**, *12*, 1351-1365.
34. Lu, T.; Chen, F. W. Multiwfn: A multifunctional wavefunction analyzer. *J. Comp. Chem.* **2012**, *33*, 580-592.
35. Crespo-Hernández, C. E.; Cohen, B.; Hare, P. M.; Kohler, B. C. R. Ultrafast excited state dynamics in nucleic acids. *Chem. Rev.* **2004**, *104*, 1977-2019.
36. Improta, R.; Santoro, F.; Blancafort, L. Quantum Mechanical Studies on the Photophysics and the Photochemistry of Nucleic Acids and Nucleobases. *Chem. Rev.* **2016**, *116*, 3540-3593.
37. Su, C.; Middleton, C. T.; Kohler, B. Base-Stacking Disorder and Excited-State Dynamics in Single-Stranded Adenine Homo-oligonucleotides. *J. Phys. Chem. B* **2012**, *116*, 10266-10274.
38. Balanikas, E.; Banyasz, A.; Douki, T.; Baldacchino, G.; Markovitsi, D. Guanine Radicals Induced in DNA by Low-Energy Photoionization. *Acc. Chem. Res.* **2020**, *53*, 1511-1519.
39. Balanikas, E.; Markovitsi, D. DNA photoionization: from high to low energies. In *DNA Photodamage: From Light Absorption to Cellular Responses and Skin Cancer*, Improta, R.; Douki, T., Eds. RSC: Cambridge, 2021; pp 37-54.
40. Saito, I.; Nakamura, T.; Nakatani, K.; Yoshioka, Y.; Yamaguchi, K.; Sugiyama, H. Mapping of the hot spots for DNA damage by one-electron oxidation: Efficacy of GG doublets and GGG triplets as a trap in long-range hole migration. *J. Am. Chem. Soc.* **1998**, *120*, 12686-12687.